Surface reactivity and layer analysis of chemisorbed reaction films in the surface-chemical environment of alkyl octadecenoates

R B CHOUDHARY[1,]*, O N ANAND[2] and O S TYAGI[3]

[1]Center for Advanced Technology (CAT), Haryana Engineering College Jagadhari, Yamunanagar, Haryana 135 003
[2]Specialties and Additives Group, Chemical and Bio-Science Division, Indian Institute of Petroleum, Mohkampur, Dehradun 248 005
[3]Spectroscopy (FTIR) Laboratory, Analytical Science Division (ASD), Indian Institute of Petroleum, Mohkampur, Dehradun 248 005
e-mail: rbchec@yahoo.co.in

Abstract. Studies on surface reactivity of substrate iron (Fe-particles) were made in the tribo-chemical environment of alkyl octadecenoates. Two alkyl octadecenoates namely ethyl octadecenoate and methyl 12-hydroxy octadecenoate, slightly different in their chemical nature, were taken for preparing the chemisorbed reaction films (CRF) at the temperature $100 \pm 5°C$. The reaction products collected in the composite (amorphous) phase were isolated into three different solvent–soluble fractions (sub-layer films) using polar solvents of increasing polar strength. The FTIR analysis of these films showed that these were primarily organic in nature and were composed of alkyl and/or aryl hydroxy ethers, unsaturated hydroxy ketones, and aromatic structures chemically linked with iron surface. These reaction films also contained large amount of iron (Fe). Further, these film fractions also showed varying thermal behaviour during thermal decomposition in the temperature range of 50–800°C when thermally evaluated in the nitrogen environment.

Keywords. Surface reactivity; chemisorbed reaction films; solvent fractionated films; surface chemical reaction.

1. Introduction

Studies on surface reactivity of metallic iron (Fe) surfaces and the kinetics for the layer analysis of Fe–O, Fe–Al, Fe–N, Fe–B and Fe–Ni systems have been of common research interest owing to their increasing utility as electronic materials, coating materials, and the materials for surface modification. However, the detailed studies for the surface reactivity and the layer analysis of metallic iron (Fe) in organic environment appear to be scanty in literature owing to its limited utility in tribological situations. Its study in composite and amorphous phase is still a matter of greater concern for researchers because a composite is often more advantageous over its constituents since it possesses sometimes high synergistic characteristics.[1] The composition across the interface region of the composite matrix is also known to vary

significantly, resulting into a broad range of bonding. The composite films formed in the trobo-chemical environment show typical surface morphology, anomalous thermal stability and random distribution of various ions, radicals or molecules in the layered compounds. The microstructure (phase and grain structure) of composite films affect a large number of mechanical, chemical and thermal properties which in turn selectively affect the surface wear.[2]
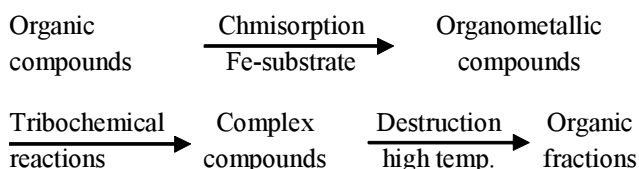
Reactivity of metallic iron (Fe) surface, in common chemical environments such as oxygen, nitrogen, chlorine, aluminum, boron, carbon, manganese, and silicon are the well established phenomena for surface modification and synergistic applications.[3–10] These studies are made for beneficiating mechanical, electrical, thermal, chemical, electrochemical, medical and many other effects. These are also highly informative for understanding the surface wear characteristics as the wear resistance and other desirable deposition of coatings are degraded

---

*For correspondence

when dilution increases.[11,12] In a recent communication, Yang reported the influence of sodium potassium (Na–K) compounds in the coating or core of the electrodes as the microstructure and wear resistance of Fe–Cr–C coatings.[13] In an another study Kotvis[14] reported the chemical effect of some well-known compounds on iron substrate such that,

$$Fe + [BO_3] \rightarrow FeO + B_2O_3$$

$$Fe + [Cl] \rightarrow FeCl_2 \quad or \quad Fe\,Cl_3.$$

Further, Forbes[15] postulated the mechanism of action for organic disulfide on iron (Fe) surfaces according to which the cleavage of the sulfur–sulfur bond occurs so that iron mercaptide is formed. It is also because of the reason that adsorbing molecules break into several fractions or species well before chemisorptions on to the metal surfaces.[16] A similar kind of study was reported by Choudhary *et al*[17] in a recent review on action mechanism of boundary lubrication additive compounds. Early study on metal–chemical reaction sometimes in the mid sixties[18,19] has already made dent mark in this direction. However, the concept of layer development and their micro-analysis appeared more explicitly in the late eighties. Kajdas[20] reported the formation of organo–metallic compounds by the reaction of organic compounds on to the metallic surfaces and the subsequent reaction products as an effect of destruction in tribo-chemical environment follows as shown below:

Organic compounds $\xrightarrow[\text{Fe-substrate}]{\text{Chmisorption}}$ Organometallic compounds

Tribochemical reactions $\xrightarrow{}$ Complex compounds $\xrightarrow[\text{high temp.}]{\text{Destruction}}$ Organic fractions
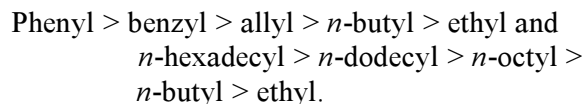
During tribo-chemical reaction, emission of low energy electron, typically known as exo-electron, has significant role to play. Rosenblum *et al* reported that apart from electron, some ions and lattice components are also emitted during mechanical deformation.[21] Further, if the energy of exoelectron is sufficiently high (> 10 eV), the interaction of electrons with chemical compounds results into formation of positive ions in the reaction;[22] $A + e^- \rightarrow A^+ + 2e^-$. However, electrons of an average energy ~ 3 eV are known to be attached to the molecules resulting into the formation of negative ions[22] such that $A + e^- \rightarrow A$. Thus the energy of exo-electron is

known to have cause marked effect on the formation of ions. Rowe *et al*[23] discussed the postulates of surface reactivity at surface boundary of metallic surfaces involving emission of exo-electron and catalytic action,

Exo electrons + Mechanical stress +
  Catalytic activity + Thermal impacts $\rightarrow$
  Surface reactivity.
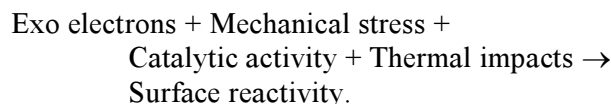
Infact, the mechanical stress tends to promote chemical reactions at solid surface and introduce chemistry. The surface reactivity of organic species also depends upon the strength of the polar groups, chemical function and their structural characteristics. The order of decreasing anti-wear activity of some of the organic species[24,25] as an effect of surface reactivity have been shown below followed as:

Phenyl > benzyl > allyl > *n*-butyl > ethyl and
  n-hexadecyl > *n*-dodecyl > *n*-octyl >
  n-butyl > ethyl.

In order to postulate the probable reactivity of chemical species with metal surfaces, it is therefore, desirable to generate surface reaction films and study their structural characteristics. These involve surface chemical reactions for preparing their inorganic, organo–inorganic, organo–metallic, intermetallic and eutectic compounds in crystalline as well as in the non-crystalline form. This may also involve a large number of analytical techniques such as IRAS (infrared reflectance absorption spectroscopy),[26–29] AES,[30–32] EXAFS,[33] NMR,[34] SEM,[35] XPS[36] and IETS (inelastic electron tunneling spectroscopy.[37] Smith[38] has recently reviewed the surface analytical science for understanding the structure and composition of anti-wear films formed in tribocontacts. However, FTIR spectroscopy is known to be the most commonly known spectroscopic technique to identify the functional groups in the reaction film of metal–chemical reactions.

Further decomposition of a surface reaction film comprising various chemical species, in the thermal environment is another significant physico–chemical characteristics observed by the surface experts. Although the detailed communications of such studies is scanty in literature. Hoveer, the decomposition of some well known class of additive compounds provide adequate information in this direction. Klauss *et al*[39] studied the differences for

thermal decomposition reaction in the gaseous and liquid phases and emphasized for controlling the secondary reaction involved. Weisner *et al*[40] reported that although neutral alkyl diaryl phosphate esters are very stable at room temperature ($\sim 25°C$) but these esters are thermally unstable at high temperature and the thermal stability is dependent on time, temperature and structure. Researchers have reported the varying postulates for the mechanism of decomposition metal organo-dithiophosphate as well. Feng *et al*[41] proposed a multi stage mechanism in which the first stage involved the formation of polymer. Their study led to the essential advantages of the experimental results for the film analysis. In the present communication, authors aim to investigate the probable mechanisms of action for surface reactivity of metallic iron (Fe) particles with alkyl octadecenoates. The study involves the formation of chemisorbed (crude or composite) reaction films in amorphous phase and subsequently their isolation in different possible sub-layer fractions using polar desorption technique.[17] Further, these are characterized by FTIR micro-analysis and the thermal analysis of sub-layer fraction has been studied using TGA technique. The emphasis is made for investigating the chemical nature of CRFs but no interest was desired for understanding the kinetic studies in the preliminary stage of investigation.

2. Experimental

2.1 *Preparation of chemisorbed reaction films (CRFs)*

The materials used involve ethyl octadecenoate ($C_{20}H_{38}O_2$), methyl 12-hydroxy octadecenoate ($C_{18}H_{36}O_3$), chloroform ($CHCl_3$), dimethylformamide (C_3H_7ON) acetic acid ($C_2H_3O_2$), xylene (C_9H_{12}), *n*-heptane (C_7H_{16}), 2N-hydrochloric acid (HCl), electrolyte grade iron (Fe) particles (100–200 mesh size powder) and light paraffin liquid (sulfur-free). The slurry of alkyl octadecenoate (5 wt%) and electrolyte grade iron (Fe) particle (7 wt%) in light paraffin liquid was refluxed in a flask continuously for eighteen to twenty 18–20 h at temperature $100 \pm 5°C$. The reaction product was filtered and washed with petroleum solvent (bp 60°–80°C) until the trace of paraffin liquid was removed. The crude film was smoothly dried at reduced pressure and temperature to make it free from washing solvent. Further, it was treated with 2N-hydrochloric acid at

the temperature slightly greater than room temperature. The wet film was dried and collected in the composite phase. A macroscopic view of the chemisorbed reaction Fe-particles has been shown in figure 1. Further, the CRF was taken inside the soxhlet apparatus and extracted with chloroform. The extraction process was continued with other polar solvents of increasing (higher) polar strength so that a large amount of film fractions could be collected. These solvent fractionated films were chloroform soluble fraction (CSF), dimethylformamide soluble fraction (DSF), acetic acid soluble fraction (ASF) and residual solvent insoluble fraction (RSF). These were typically termed as primary layer film, intermdiate layer film and deep layer film. Lastly, residual film substrate was left behind the extraction. These film specimens namely, chemisorbed reaction (composite) films and the three solvent fractions were subjected for analytical study like elemental composition, chemical composition, probable empirical formula as shown in the table 1 using FTIR spectroscopic technique for the identification of chemical moieties and functional groups. The yield (weight percent) for different film fractions are shown in the table 2. The elemental contents in the derived films are shown in the table 1. However, the trends in the elemental content of solvent fractionated films are shown in table 3.

2.2 *Thermal analysis*

Thermal analysis of sub-layer film specimens of methyl 12-hydroxy octadecenoate was carried out using thermo gravimetric analysis (TGA) techniques. The analysis was selectively conducted for methyl 12-hydroxy octadecenoate specimen as it comprises higher order of functional groups as compared to ethyl octadecenoate. Small amount of film
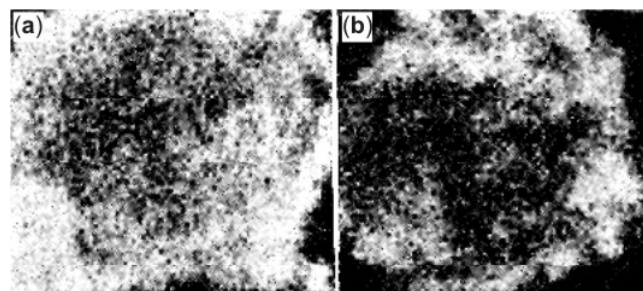

Figure 1. Chemisorbed reaction of Fe-particles in the tribo-chemical environment (**a**) ethyl octadecenoate, and (**b**) methyl 12-hydroxy octadecenoate.

Table 1. Elemental constitution of solvent fractionated sub-layer films.

Films origin	Source of additives	C (%)	H (%)	O (%)	Fe (%)	Empirical formula
CSF	EOL	79·48	06·14	07·43	08·59	$C_{56.6}H_{52.2}O_4Fe$
	MRO	84·84	07·06	07·10	00·86	$C_{16}H_{16}OFe$
DSF	EOL	85·69	06·65	03·56	04·16	$C_{97.5}H_{91}O_3Fe$
	MRO	67·08	05·52	09·96	17·44	$C_{18}H_{18}O_2Fe$
ASF	EOL	58·91	04·04	16·29	20·76	$C_{13.2}H_{10.9}O_{2.8}Fe$
	MRO	67·67	05·26	05·87	21·10	$C_{15}H_{14}OFe$
RSF	EOL	40·23	02·67	30·43	26·68	$C_7H_{5.6}O_4Fe$
	MRO	48·30	03·35	10·34	38·01	C_6H_5OFe

Table 2. Yield analysis (wt%) of solvent fractionated (sub-layer) films.

Additives	CRF	CSF	DSF	ASF	RSF
EOL	9·40	0·70	2·20	2·80	3·70
MRO	9·20	0·80	1·80	2·80	3·80

Table 3. Trends in elemental content in chemical analysis of sub-layer films

Additives	Elemental contents	Order of sub-layer films
EOL	Iron (Fe)	RSF > ASF > CSF > DSF
	Carbon (C)	DSF > CSF > ASF > RSF
	Oxygen (O)	RSF > ASF > CSF > DSF
	Hydrogen (H)	DSF > CSF > ASF > RSF
MRO	Iron (Fe)	RSF > ASF > DSF > CSF
	Carbon (C)	CSF > ASF > DSF > RSF
	Oxygen (O)	RSF > DSF > CSF > ASF
	Hydrogen (H)	CSF > DSF > ASF > RSF

EOL, Ethyl octadecenoate and MRO; methyl 12-hydroxy (OH) octadecenoate

specimen was taken for thermal evaluation. The film specimens were made moisture free well before subjecting for thermal analysis. The analysis was conducted in nitrogen environment with well adjusted flow rate of nitrogen in the temperature range of 50–800°C with the heating rate of 10°C per minute. The corresponding weight reduction (loss) in percent (%) was recorded as shown in the thermograms. However, no interest was taken for analysing the chemical nature of gaseous contents evolved in the nitrogen environment during thermal decomposition of the solvent fractionated film specimens.

2.3 *Structural characteristics*

Structural characteristics of sub-layer film specimens were carried out by FTIR spectroscopy in accordance with the two different class of alkyl octadecenoates. FTIR absorption spectra of as-prepared CRFs on iron substrate were recorded using Perkin Elmer Model 2000 FTIR spectrometer equipped with a microscope, fitted with a movable X–Y stage, a micro ATR crystal and a MCT detector. A piece of sample was pressed in a diamond anvil to flatten it before mounting on the stage of microscope. The surface of particle was scanned to obtain its microscopic image in order to select the sites suitable for recording the spectra. The spectra were recorded in the reflectance mode by co-adding 580 cm^{-1} scans of resolution in 4000–580 cm^{-1} region. The detailed structural analysis of solvent-fractionated films were carried out by IR absorption spectra of CSF, DSF, ASF, and RSF of corresponding CRFs. IR spectral characteristics, assignments and description of significant absorption bands have

Table 4. IR spectral characteristics, assignments and description of significant absorption bands

Additives	Regions	CSF-Film	DSF-Film	ASF-Film	RSF-Film
EOL	3500–2000 cm^{-1}	2963 (*s*), 2917 (*s*) 2849 (*s*)	3400 (*s*), 2992 (*s*) 2775 (*s*), 2448 (*m*)	3434 (*s*), 2925 (*s*) 2828 (*s*)	3448 (*s*), 2980 (*m*)
	1800–1300 cm^{-1}	1608 (*w*), 1596 (*w*), 1460 (*w*), 1413 (*w*)	1772 (*s*), 1630 (*m*), 1467 (*s*)	1613 (*m*), 1480 (*m*), 1408 (*w*), 1384 (*m*)	1578 (*s*), 1543 (*s*), 1446 (*s*), 1430 (*s*)
	1300–500 cm^{-1}	1261 (*s*), 1093 (*s*) 1020 (*s*) 865 (*m*), 800 (*s*) 662 (*w*), 477 (*s*)	1027 (*m*) 1020 (*m*) 888 (*m*)	1144 (*m*)1 1080 (*m*), 1020 (*m*), 800 (*w*), 703 (*m*) 700 (*m*) 466 (*s*)	1030 (*m*), 980 (*w*), 815 (*w*) 664 (*s*), 615 (*s*) 514 (*m*), 505 (*m*)
MRO	3500–2000 cm^{-1}	3453 (*m*), 2927 (*s*), 2855 (*s*), 1948 (*w*)	3409 (*s*), 3013 (*s*) 2779 (*s*)	3017 (*w*) 2963 (*w*) 2828 (*w*)	3400 (*m*) 2929 (*w*) 2828 (*w*)
	1800–1300 cm^{-1}	1744 (*m*), 1715 (*m*) 1602 (*w*), 1456 (*s*) 1413 (*s*), 1377 (*s*)	1703 (*ms*), 1620 (*s*) 1466 (*s*) 1413 (*m*)	1724 (*w*) 1609 (*m*) 1515 (*s*) 1447 (*s*) 1352 (*m*)	1719 (*w*), 1556 (*s*) 1444 (*s*)
	1300–500 cm^{-1}	1261 (*s*), 1100 (*s*) 1022 (*s*) 860 (*s*) 771 (*s*)	1020 (*s*), 835 (*w*)	661 (*m*) 586 (*m*) 517 (*w*), 475 (*w*)	1050 (*w*), 1025 (*w*) 801 (*w*) 663 (*w*) 617 (*m*) 539 (*w*) 504 (*s*)

been shown in table 4. However, no spectra have been depicted as such except taking their prominent peak values.

3. Results and discussions

3.1 *CRF of ethyloctadecenoate*

The FTIR spectrum for CSF of ethyl octadecenoate showed resolved bands of medium-to-strong intensity assigned to (1) νC–H stretching vibrations of C–CH$_3$ at 2963 cm^{-1} and CH$_2$ at 2917 cm^{-1} (2) νC–O stretching vibrations of aryl at 1261 cm^{-1}, alkyl at 1093 cm^{-1} and cyclic ethers at 1020 cm^{-1} and (3) γOH out-of-plane bending vibrations of tetra substituted benzene rings at 865 and 800 and = CH.CH$_3$ group at 661 cm^{-1}. Weak absorption bands were also observed that were assigned to νCH=CH at 3030 cm^{-1} and ν_β C=C of aromatic at1596 cm^{-1} ν_s CH$_2$ at 2489 cm^{-1}, δ = CH$_2$ at 1460 cm^{-1} and ω = CH$_2$ of methylene at 1413 cm^{-1}, conjugation in C=C or C=O at 1596–1500 cm^{-1}. These assignments suggest that the CSF consist of highly substituted condensed ring aromatic structure with alkyl and cyclic ether linkages with methylene and olefinic groups. The DSF showed broad bands of medium-to-strong intensity assigned to intermolecularly bonded hydroxyl groups (νOH) with maxima at 3540–3400 cm^{-1} region, unsaturated νC–H band at 3000 cm^{-1}, ole-

finic γ = CH at 888 cm^{-1}, unsaturated νC–OH at 1020 cm^{-1}, allene νC=C at 2775 cm^{-1}, 2448 cm^{-1} and 1632 cm^{-1}, ketonic νC = O at 1712 and 1632 cm^{-1}, unsaturated cyclic 6 and 7 member ring and alkyl δ_s CH$_2$ at 1467 cm^{-1}. Thus DSF is known to be composed of mainly hydroxy ketone and diketones consisting saturated cyclic rings unsaturated moieties such as linear polyenes. The ASF showed several medium-to-strong intensity broad bands with few partially resolved shoulder bands of weak-to–medium intensity assigned to conjugated hydroxy cations at 3450, 1744 and 1666 cm^{-1} attached to unsaturated and mono-substituted aromatic ring structure at 1613, 1150 and 650 cm^{-1} and anchored to the iron (Fe) surface through carboxylate linkages at the 1416, 1406, 1100–800 cm^{-1}. The bands of C.CH$_3$ at 2963 cm^{-1} and CH$_3$ at 1384 cm^{-1} in absence of the bands (CH$_2$)$_n$ $n > 4$ near 724 cm^{-1} suggest the presence of some branched alkane function with the short alkyl chain. The RSF showed medium to strong bands at 3448, 2980, 1368, 664 and 615 cm^{-1} very strong absorption bands at 1578, 1583, 1446 and 1430 cm^{-1} weak bands at 1430, 815, 514, 505 cm^{-1}. These assignments suggest that the RSF contains mainly aromatic hydroxy cations/quinones having highly condenced aromatic ring structures chelated to large amount of iron. Thus, ethyl octadecenoate reacts with the iron (Fe) surfaces through its ester carbonyl groups followed by the abstraction of

the hydrogen from the alkyl chain and the formation of the precursor leading to the generation of the hydroxy cations and condensed ring aromatic structures that are linked to the iron surface through C–O bonds.

3.2 *CRF of methyl 12-hydroxy octadecenoate*

The FTIR spectrum of CSF showed annulment of absorption bands of ester and long chain alkyl functions at 1742 cm^{-1} and 729 cm^{-1}. Strong-to-medium intensity peaks due to stretching and bending vibration of alkyl C–H were present at 2927, 2856, 1456 and 1377 cm^{-1}. New strong peaks also occurred at 1261, 1097 and 1024 cm^{-1} attributed to stretching vibration of C–O and C–O–C in aryl/unsaturated alkyl ethers. The peaks at 1456 (δCH$_2$), 1413 cm^{-1}

(ωCH$_2$) and at 1097 cm^{-1} (ν_{as} C–O) were indicatives of cyclic ethers. Medium to strong intensity absorption at 1602, 1413, 803 and 702 cm^{-1} indicated the presence of both mono and poly substituted aromatic species. Thus, it is inferred that CSF comprises primarily condensed ring aromatic structures with short alkyl chain linked through ethereal oxygen. FTIR spectrum of DSF showed strong absorption bands at 3409 cm^{-1} and 1020 cm^{-1} assigned to νO–H and νC–C respectively suggesting the presence of secondary alcohol. Two strong peaks for νC=O at 1708 and 1620 cm^{-1}, and three weak bands for νC–O at 1248, 1166 and 1087 cm^{-1} jointly indicated the presence of unsaturated ketones conjugated with hydroxy groups. There are strong to medium intensity peaks of νCH$_2$ at 3013 cm^{-1}, νC=C conjugation at
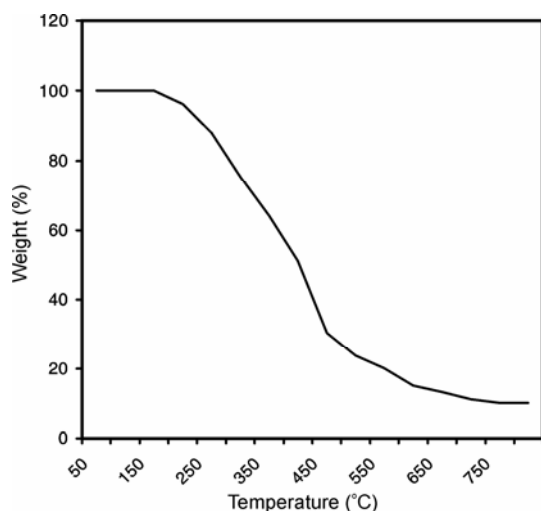
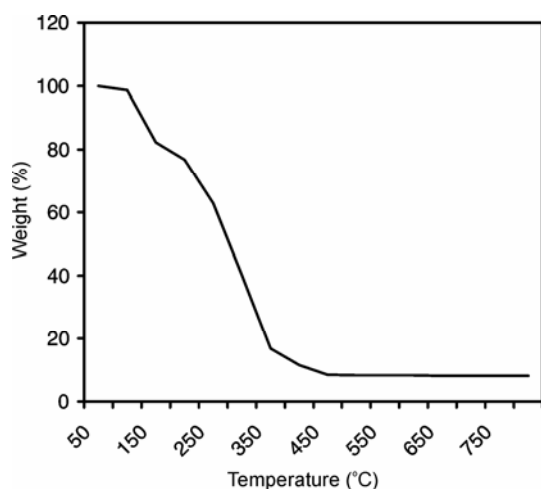**Figure 2.** TGA of chloroform soluble fraction (CSF).
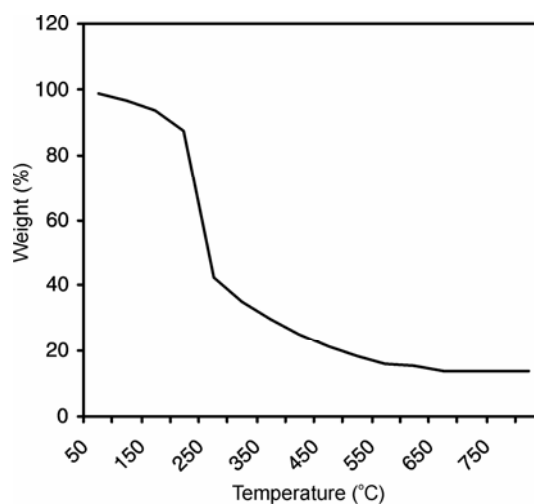
Figure 3. TGA of DMF soluble fraction (DSF).
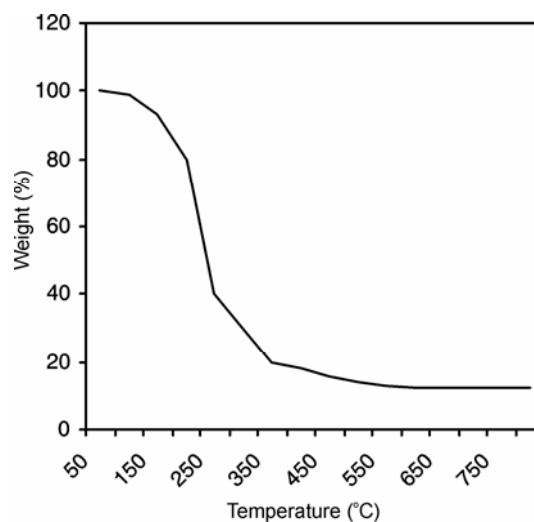
Figure 4. TGA of acetic acid soluble fraction (ASF).

**Figure 5.** TGA of residual solvent insoluble fraction (RSF).

1620 cm^{-1} and βCH$_2$ at 1413 cm^{-1} of alkenes along with wide δCH$_2$ at 1465 cm^{-1} of alkyl groups suggest that DSF comprises mainly unsaturated hydroxy ketones with short alkyl chains. FTIR spectrum of ASF showed weak CH bond of alkyl group at 2963 and 2815 cm^{-1} and annulment of their bending and rocking vibration. It showed several peaks of varying intensity assigned to aromatics at 3017, 1609, 1515, 661, 585, 517 and 475 cm^{-1}, νC=O and νC–O of carboxylic groups at 1447 and 1027, ωCH$_2$ at 1352 cm^{-1}, and weak absorption of ketonic νC=O at 1724 cm^{-1}. These analysis infer that ASF contain aromatic species containing some ketonic fractions chelated to iron through a large number of carboxylate functional groups. FTIR spectrum of RSF showed only a few strong-to-medium intensity bands at 3467 and 3400 cm^{-1} assigned to νC–H, δO–H, at 1446, νC=O at 1626 cm^{-1}, ωCH$_2$ in chain at 1351 cm^{-1}, νC=O of COO$^-$ at 1446 cm^{-1} and different modes of vibration of condensed aromatic rings at 1626, 1554, 810, 666, 618 and 505 cm^{-1}. These analysis suggest that RSF is composed of condensed aromatic structures with carbonyl and hydroxy groups and carboxylate substituents linking with iron. It is, therefore, recognized that methyl 12-hydroxy octadecenoate reacts with iron surfaces more effectively than ethyl octadecenoate and the reaction occurs through ester and hydroxyl groups with the parallel participation of alkyl chains in the reaction.

3.3 *Yield analysis*

The yield of CRF under the experimental condition was about one-fourth (1/4) to one-sixth (1/6) of the mass of the alkyl octadecenoates (esters). The derivatization of esters had a marginal (2–2·5%) detrimental effect of the yield. The fractionations of CRFs by soxhelet extraction produced almost similar yield pattern for the two different chemical species. The yield of each solvent fraction increased with the polarity of solvents used. The solvent insoluble fractions was 33–41 weight percent. The yield weight percent for the solvent fractionated films is shown in the table 2. The elemental analysis showed decreasing order trends in the elemental constituents (Fe, C, O, H) of film fractions as shown in table 3. This suggested that a major portion of each reaction film was insoluble or sparsely soluble even in highly polar solvent (acetic acid) which also contained maximum weight percent of iron (Fe).

3.4 *Probable modes of action*

The alkyl octadecenoates employed appear to impart, C–C, C–O, C=O, C–O–C and O–H linkages. The long-chain of (CH$_2$)$_n$ in these compounds condenses into cyclic and aromatic structures. The three major reaction sites namely carbonyl group, hydroxyl group and unsaturated double bond in C-18 linkages causes functionalization. The presence of hydroxyl group allows hydrogen bonding with soap molecules, which causes the formation of crystalline aggregates. The double bond causes the bulky portion of long chain to reside on the same geometric side of the unsaturated linkages. This allows the electron rich unsaturated bond to intimately contact the surfaces and accounts for the wetting ability. The carboxyl group causes to occur the reactions such as amidification, trans-esterification and hydrogenation. Other typical reactions such as addition, epoxidation and polymerization occur to produce many intermediate compounds for further functionalization.
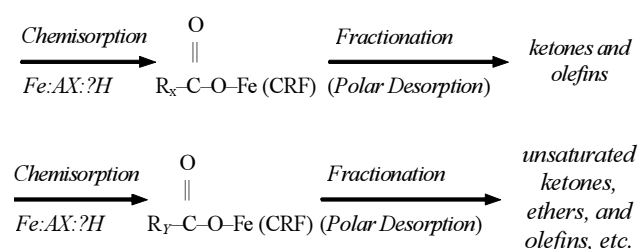
where, $AX(X) \rightarrow$ Ethyl octadecenoate; $AY(OH) \rightarrow$ Methyl-12-hydroxy octadecenoates and $?H \rightarrow$ Heat of surface-chemical reaction.

3.5 *Thermal analysis*

The different solvent fractioned sub-layer films of methyl 12-hydroxy octadecenoate origin were subjected for thermal analysis. Multi-stage decomposition (degradation) occurred during thermal evaluation process. Most of these films lost their thermal stability in the temperature range of 200–400°C. The CSF of methyl 12-hydroxy octadecenoate shows better stability during thermal decomposition. The thermal stability of these sub-layer films lie in the order of CSF > DSF > ASF > RSF respectively. CSF, DSF, ASF and RSF of methyl 12-hydroxy octadecenoate decomposed in the temperature range of 200–700°C, 100–400°C, 100–500°C and 100–400°C respectively with their corresponding weight loss of 90%, 92%, 86%, and 88%. Notably ASF and RSF show abrupt decomposition as compared to

CSF and DSF. Such an anomaly in their thermal behaviour is known to be incurred owing to their varying structural characteristics and functional behaviour of the film specimens under evaluation.

4. Conclusion

The substrate iron (Fe) particles undergo extensive surface–chemical reactions with alkyl octadecenoates under the experimental condition of tribo-chemical reaction. It causes to produce numerous surface chemical bonding and provide O–H, C–C, C–O, C=O, and C–O–C linkages. The chemisorbed reaction film (CRF) thus formed is composite layers and complex mixtures of polymeric organic and inorganic compounds of iron (Fe). These films are chemically soluble in the hydrocarbon solvents of increasing polar strength. These films chelate maximum amount of iron, and form highly conjugated hydrogen bonded structures. However, the iron derivative of methyl 12-hydroxy octadecenoate form major part of chemisorbed reaction films in the surface–chemical (Fe : AX : ?H) environment. Further, CSF stands thermally more stable among the varying categories of sub-layer films of methyl 12-hydroxy octadecenoate origin.

Acknowledgements

References

1. Eustathopoulos N, Nicholas M G and Drevet B 1999 (NY: Pergamon) p. 93
2. Bull S J 1999 *Wear* **233** 412
3. Nayak S, Meyer H M and Dahotre N B 2004 *Surface Eng.* **20** 48
4. Dwivedi D K 2004 *Surface Eng.* **20** 87
5. Parezanovic I and Spiegel M 2004 *Surface Eng.* **20** 285
6. Lin M L, Zhou H L, Chen Y R and Jia Y Q 2005 *Mater Chem. Phys.* **80** 289
7. Tsay P C-C Hu and C-K Wang 2005 *Mater. Chem. Phys.* **89** 275
8. Ratajski J I 2004 *J. Mater. Res. Adv. Tech.: Z. Metallkd* **95** 9
9. Peng K, Liu F, Fu D, Huang Z, Xu F and Du Y 2005 *Mater. Chem. Phys.* **89** 138
10. Li, Y-J, Wang J, Yin Y-S and Ma H-J 2004 *Mater. Soc. Technol.* **20** 1484
11. Francis J A 2002 *Sci. Tech. Weld.* **7** 331
12. Kotechki D J and Ogborn J S 1995 *Weld. J.* **7** 269
13. Yang J H 1995 *Weld. J.* **2** 103
14. Kotvis P V 1986 *Lubrication Eng.* **42** 363
15. Forbes E S and Allum K G 1967 *J. Inst. Petrol.* **53** 173
16. Buckley H (ed.); 1987 *CRC Handbook of lubrication*, p. 28
17. Chudhary R B and Jha M K 2004 *Lubri. Sci.* **16** 205
18. Edward E W and Davey W 1958 *Wear* **1** 291
19. Sakurai T, Ikeda S and Okabe H 1962 *ASLE Trans.* **5** 67
20. Kajdas C 1984 *Lubri. Sci..* **34** 261
21. Rosenblum, B, Braulich P and Mimmel L 1977 *J. Appl. Phys.* **48** 5262
22. Von A M, Steinfelder K and Tummler R 1971 (Berlin: Springer Verlag) p. 121
23. Rowe C N and Murphy W R 1977 *Tribo Work* (Washington DC: NSF) p. 327
24. Allum K G and Ford J F 1965 *J. Inst. Petr.* **51** 497
25. Allum K G and Forbes E S 1967 *J. Inst. Petrol* **5** 521
26. Willermate A, Pieprzak J M, Dailey D P, Carter R O, Lindsay N E, Haak L P and deVrieS J E 1991 *ASME J. Tribo.* **113** 38
27. Harrison G and Brown P 1991 *Wear* **148** 123
28. Willermate P A, Carter R O and Boulos E N 1992 *Tribo. Int.* **25** 371
29. Weinmin L, Ganzhu G, Pingyu Z and Qunji X 1997 *Lubri. Sci.* **10** 67
30. Palermo T, Giasson S, Buffeteau T, Desbat B and Turlet J M 1996 *Lubri. Sci.* **8** 119
31. Chen C, Dong J and Chen G 1996 *Mocaxue Xuebao* **16** 247
32. Barkshire I R, Pruton M and Smith G C 1995 *Appl. Sur. Sci.* **84** 331
33. Smith G C and Bell J C 1999 *Appl. Sur. Sci.* **144** 222
34. Martin J M, Belin M and Mansot J L 1986 *ASLE Trans.* **29** 523
35. Schuetzle D, Shyu R O J, Dickie R A, Halubka J and McLintyre N S 1986 *Appl. Spectro.* **40** 641
36. Pidduck A J and Smith G C 1997 *Wear* **212** 254
37. Smith G C 2000 *J. Appl. Phys.* **D33** 187
38. Wooten D L and Hughes D W 1987 *Lubr. Eng.* **43** 736
39. United State Patent No. 6936906
40. Weisner U, Floudas G and Ulrich R 1999 *J. Chem. Phys.* **110** 652
41. Feng J, Pham H, Macdonald P, Winnik, M A, Geurts J M, Zirkzee H, Vanes S and German A L 1998 *J. Coatings Technol.* **70** 57